Pharmacogn. Res., 2025; 17(1):115-125.
https://www.phcogres.com

Original Article

# *In silico* Exploration of *Gmelina asiatica* for Multitarget Neuroprotection in Alzheimer's Disease

**Komal Rajesh Andarghiske[1], Kancharla Bhanukiran[2], Rasha Ksirri[1,3], Siva Hemalatha[1,*]**

[1]Department of Pharmaceutical Engineering and Technology, Indian Institute of Technology (Banaras Hindu University), Varanasi, Uttar Pradesh, INDIA.
[2]Department of Pharmacognosy, GITAM School of Pharmacy, GITAM (Deemed to be University), Visakhapatnam, Andhra Pradesh, INDIA.
[3]Department of Pharmacognosy, Faculty of Pharmacy, University of Damascus, Damascus, SYRIA.

## ABSTRACT

**Background:** *Gmelina asiatica,* commonly known as Asian Bushbeach, has traditionally been used for neurological disorders. **Objectives:** To identify the phytoconstituents activity in Alzheimer's disease through *in silico* approach. **Materials and Methods:** The following targets AChE, BACE1, GSK-3, and TACE1 were selected based on AD pathophysiology for *in silico* studies. The listed phytoconstituents were docked and MD simulations were carried out using Auto Dock and Desmond-maestro, respectively. Further, DFT studies were performed using Gaussview software. **Results:** Among all listed ligands, isorhoifolin was identified as the most effective compound based on binding scores of AChE (-10.9 kcal/mol), BACE1 (-10.2 kcal/mol), GSK-3 (-9.7 kcal/mol), and TACE1 (-9 kcal/mol). Further, molecular dynamics simulations of BACE1-isorhoifolin and AChE-isorhoifolin complexes demonstrated stability for up to 200 ns. Density Functional Theory (DFT) studies indicated isorhoifolin have energy gap of -0.162 eV along with that electrostatic potential surface map indicates its good reactivity and charge distribution. Additionally, ADMET analysis confirmed that isorhoifolin have drug-likeness properties and safe for human biological system. **Conclusion:** These study findings suggest that isorhoifolin from *Gmelina asiatica* may have potential anti-Alzheimer's activity meriting further biological evaluations.

**Keywords:** Alzheimer's disease, DFT, *G. asiatica*, Isorhoifolin, Molecular Dynamics, Multitargeted approach.

**Correspondence:**
**Dr. Siva Hemalatha**
Professor and Head, Department of Pharmaceutical Engineering and Technology, Indian Institute of Technology (Banaras Hindu University), Varanasi-221005, Uttar Pradesh, INDIA.
Email: shemalatha.phe@itbhu.ac.in
ORCID ID: 0000-0002-2928-1446

**Received:** 22-09-2024;
**Revised:** 29-10-2024;
**Accepted:** 03-12-2024.

## INTRODUCTION

Alzheimer's disease is a neurodegenerative disorder characterized by progressive loss of neurons, leading to gradual memory impairment and cognitive dysfunction. Its pathophysiology involves a complex interplay of molecular and cellular mechanisms.[1] Abnormal accumulation of β-Amyloid peptides (Aβ) is considered an early event in AD. These peptides are derived from the proteolytic cleavage of Amyloid Precursor Protein (APP) by β-site APP Cleaving Enzyme 1 (BACE1).[2] Alongside Aβ, Glycogen Synthase Kinase-3 (GSK-3) plays a pivotal role, particularly GSK-3beta, contributing to the formation of Paired Helical Filament (PHF)-tau, a key component of Neurofibrillary Tangle (NFT) deposits associated with neuronal dysfunction and neurodegeneration in AD.[3] Additionally, Tumour Necrosis Factor α (TNF-α) emerges as a significant inflammatory cytokine implicated in AD pathogenesis. Produced by various cell types, including neurons and glia, TNF-α promotes inflammatory responses, potentially inducing Aβ production and contributing to glial cell activation.[4] Studies using transgenic mice have shown that inhibition of TNF-Receptor (TNFR) signalling can reduce brain amyloid plaques and Aβ levels. Clinical investigations also suggest modulating TNF-α expression may improve cognitive function in AD patients.[5] Furthermore, inhibition of Acetylcholinesterase (AChE) will result in the reversal of acetylcholine deficiency, which is among the major events in the pathology of AD expressed in the cholinergic hypothesis.[6] These insights underscore the multifactorial nature of AD pathology, implicating processes involving Aβ accumulation, tau pathology, and inflammatory responses, thus presenting potential therapeutic targets.[7]

The current treatments available in the market for the treatment of AD are donepezil, rivastigmine (AChE inhibitor), and memantine (NMDA blocker). These marketed drugs exert their pharmacological actions by targeting specific aspects of AD pathophysiology, such as acetylcholinesterase inhibition, deposition of amyloid beta protein in the cerebral cortex, tau phosphorylation.[8] New approaches for AD treatment include inducing P-gp for amyloid beta clearance and inhibiting NLRP3

**DOI:** 10.5530/pres.20251950

inflammasome activation.[9] However, these efforts failed in clinical trial phases.[10] This available treatment in the market provides only symptomatic relief and fails to halt the progression of the disease.[11] The outcomes of these undesirable attempts highlight the inadequacy of single-targeting approaches, indicating the need for a multitargeted approach.[12] Polypharmacology, which involves either the administration of a combination of multiple drugs that act on different targets of the pathophysiology of disease or identifying one potential candidate that offers a favourable effect on multiple targets.[13] While the latter strategy may offer a better chance of success, identifying such a candidate is challenging. Botanical drugs or natural products known for their multiple pharmacological activities gives a unique opportunity for multitargeted therapy.[14]

The plant is *Gmelina asiatica*, commonly known as Asian bushberry, belonging to the family Lamiaceae. It has been valued in traditional medicine because of its several health benefits. Extracts of this plant have shown anti-haemorrhoids, anti-arthritis, antipyretic, anti-diabetic, antioxidant, anxiolytic, and neuroprotective effects.[15] Previous studies suggest that administration of methanolic extract of leaves at a dose of 400 mg/kg has shown a decrease in amyloid beta production, accompanied by improved memory function in rodents.[16] The reported phytoconstituents were listed in the Figure 1. The history of its traditional usage combined with documented health benefits and scientific research spanning two to three decades provides compelling reasons to explore *Gmelina asiatica* for its potential in AD, indicating a strong possibility for its translation to a modern drug.[17]

Molecular docking and molecular dynamics simulation have emerged as useful techniques for screening a large number of phytochemicals and identifying hit candidates.[18] Additionally, Density Functional Theory (DFT) is valuable in exploring the electronic properties of phytoconstituents relevant to their pharmacological effect.[19] Despite *Gmelina asiatica*'s evident neuroprotective activity, there is a limitation that which phytoconstituents are the responsible for the activity was not explored.[20] Therefore, the present study aims to explore the potential of phytoconstituents of the leaf part of the plant through molecular docking. Furthermore, molecular dynamics simulation and DFT analyses are performed to elucidate the identified phytoconstituent's stability and quantum chemical properties.

## MATERIALS AND METHODS

### Docking studies

#### *Retrieval of proteins and ligands*

The Crystal structure of BACE1 in complex with amino oxazoline xanthene 9l with PDB ID: 4FRJ, Crystal structure of human acetylcholinesterase in complex with ((6-((2E,4E)-5-(benzo[d][1,3]dioxol-5-yl)penta-2,4-dienamido)hexyl) triphenylphosphonium bromide) with PDB ID: 6ZWE, the crystal structure of Glycogen synthase kinase 3 in complex with inhibitor with PDB ID:1Q5K, Crystal structure analysis of the TNF-α Converting Enzyme (TACE) in complex with Aryl-sulphonamide with PDB ID:2OI0 were retrieved from the RCBS database.[21] The proteins pdb files obtained from the database underwent various steps involving the addition of polar hydrogen, merging non-polar hydrogen, adding Colman charges, and removing water molecules and unwanted residues using auto-dock and discovery studio visualizer software. The proteins were then assigned an AD4-type radius, and the conversion of pdb files to pdbqt format for both target proteins and ligands was carried out in the Auto Dock. Subsequently the PDB structures of the phytoconstituents were retrieved from the IMMPAT (Indian medicinal plants phytochemistry therapeutics database) database, with their conversion to the PDBQT form also done in AutoDock software. After completing these steps, the prepared PDBQT files of proteins and ligands were imported into AutoDock for further grid parameter fixation studies. Grid parameters were set by targeting specific amino acids in the active sites: for BACE1 chain A, the targeted amino acids were Asp32, Tyr71, Asp228, and Gly230; for AChE chain: A, Tyr72, Tyr124, Val294, and Asp349; for GSK3 chain A, Ile62, Ala83, Asp133, and Leu188; and for TACE chain A, Thr347, Leu348, Gly349, Leu350, Leu401, Val402, Glu406, Val434, and Ala439. The grid size and position were validated as follows: for BACE1, grid size (X=35.40, Y=46.95, Z=84.96) and grid position (X=54.63, Y=65.39, Z=47.26); for AChE, grid size (X=125.5, Y=27.44, Z=-2.94) and grid position (X=72.3, Y=56.06, Z=64.33); for GSK3, grid size (X=25.36, Y=37, Z=8.293) and grid position (X=40, Y=40, Z=40); and for TACE, grid size (X=38.697, Y=27.474, Z=12.571) and grid position (X=40, Y=40, Z=40). A 100-run genetic algorithm was set, with docking parameters marked as default, followed by the assignment of docking through the Lamarckian genetic algorithm.[22] The ligands were then docked against the target proteins (BACE1, AChE, GSK3, and TACE). The results, in both 2D and 3D, were analysed using Discovery Studio Visualizer.[23]

### Docking validation

The SMILES of the ligand and receptor proteins, which had the highest binding energy, were used to generate decoys via the Database of Useful Decoys; Enhanced (DUD-E). These decoys were then docked using AutoDock Vina. A receiver operating characteristic (ROC) curve was produced from the docking results, and the Area under the Curve (AUC) was calculated using simple ROC analysis.

### Molecular dynamic simulation studies

The molecular dynamics studies were conducted using the Desmond (Maestro-Desmond) software tool. The binding interaction profile and stability of the docked ligand, which exhibited the highest binding energy with a favourable interaction

profile, were analysed in relation to its target proteins. The studies employed the Amber 18 suite within the PMEMD module. The refined system was solvated in a cubic box containing TIP3P water molecules to create an aqueous environment, and 0.15 M NaCl was added to replicate the ionic strength of physiological conditions. The simulation was carried out at a temperature of 310 K and a pressure of 1 bar, maintaining constant volume and temperature (NPT ensemble) under periodic boundary conditions.[24] Before running the MD simulation, the system was relaxed. The 200 ns MD simulations were then executed, and the results were evaluated using RMSD and RMSF interactions. RMSD plots for the Cα atoms were generated for both the protein and the ligand-bound protein to assess the relative stability of the ligand within its binding pocket using Maestro Schrödinger.[25]

### Density Functional Theory (DFT) studies

The compound structure, which showed the highest binding energy in docking studies among all phytoconstituents were analysed in molecular dynamics followed by DFT studies. Its structure was optimized using B3LYP/6-311G (d, p) basis sets with Gaussview 6.0.16 software. The HOMO-LUMO energy gap and orbital energies were determined using this optimized structure. The GaussSum 3.0 software was employed to generate the HOMO-LUMO energy gap spectrum of the Density of State (DOS). Additionally, the MEP surface, Mulliken charge analysis, bond lengths, and bond numbers were calculated using the optimized ligand structure with the B3LYP/6-311G (d,p) basis sets.[26]

### ADMET studies

Further, the compound structures' drug-likeness, ADME, and toxicity parameters were predicted virtually through pkCSM software.

## RESULTS AND DISCUSSION

### Molecular docking studies

#### *Molecular docking studies on target proteins*

The docking studies were performed on phytoconstituents in the leaf of the plant within the active sites of target proteins[27] (Table 1). For BACE1, the constituents showed binding energies between -7.4 kcal/mol to -10.2 kcal/mol, in which isorhoifolin found to have the highest binding energy with -10.2 kcal/mol and formed interactions with surrounding amino acid residues at active sites of BACE1 such as Asn233 (H-bond), Gly230 (H-bond), Asp32 (H-bond), Val332 (Alkyl bond), Thr232 (Vander Waals bond). The Asn233 (H-bond), Gly230 (H-bond), Asp32 (H-bond), Val332 (Alkyl bond), Thr232 (Vander Waals bond). These ligand-protein binding interaction of isorhoifolin was depicted in Figure 2A, whereas phytoconstituents docked at AChE active site showed binding energies between -7.6 kcal/mol to -10.9 kcal/mol and subsequently isorhoifolin has highest binding energy of -10.9 kcal/mol and formed interactions with

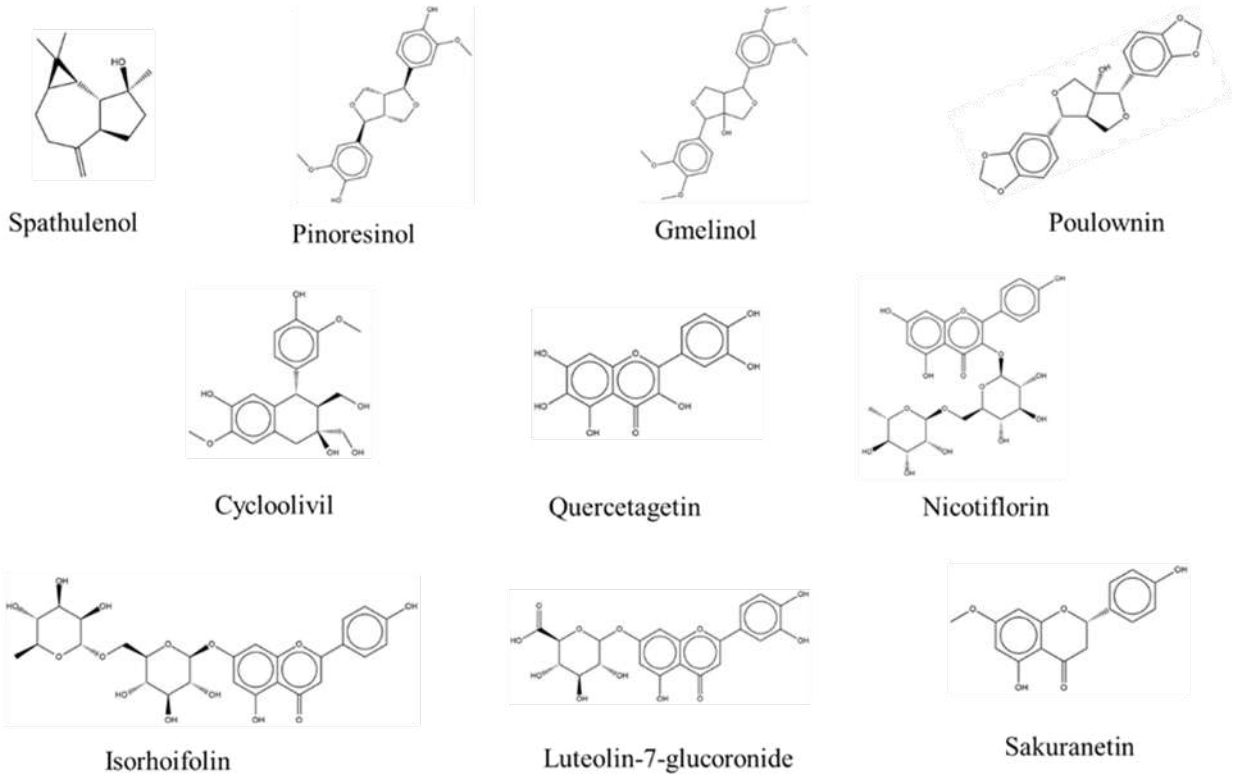


**Figure 1:** Structures of phytoconstituents from *Gmnelia asiatica.*

**Table 1: Binding energies of phytoconstituents with target protein receptors of AD.**

| Sl. No. | Phytoconstituents | AChE (kcal/mol) | (BACE-1) (kcal/mol) | (GSK-3) (kcal/mol) | TACE (kcal/mol) |
|---|---|---|---|---|---|
| 1 | Cycloolivil | -7.6 | -7.4 | -7.2 | -7.5 |
| 2 | Spathulenol | -7.9 | -7.5 | -7.5 | -6.8 |
| 3 | Nicotiflorin | -9.1 | -9.9 | -9 | -8.5 |
| 4 | Gmelinol | -9.3 | -7.8 | -7.8 | -8.5 |
| 5 | Quercetagetin | -9.3 | -8.4 | -8.5 | -8.9 |
| 6 | Pinoresinol | -9.4 | -8.5 | -8.5 | -8 |
| 7 | Sakuranetin | -9.7 | -8.4 | -8.5 | -8.5 |
| 8 | Luteolin-7-glucoronide | -9.9 | -10.4 | -9.6 | -8.8 |
| 9 | Poulownin | -10.8 | -9.4 | -8.8 | -8.2 |
| 10 | Isorhoifolin | -10.9 | -10.2 | -9.7 | -9 |

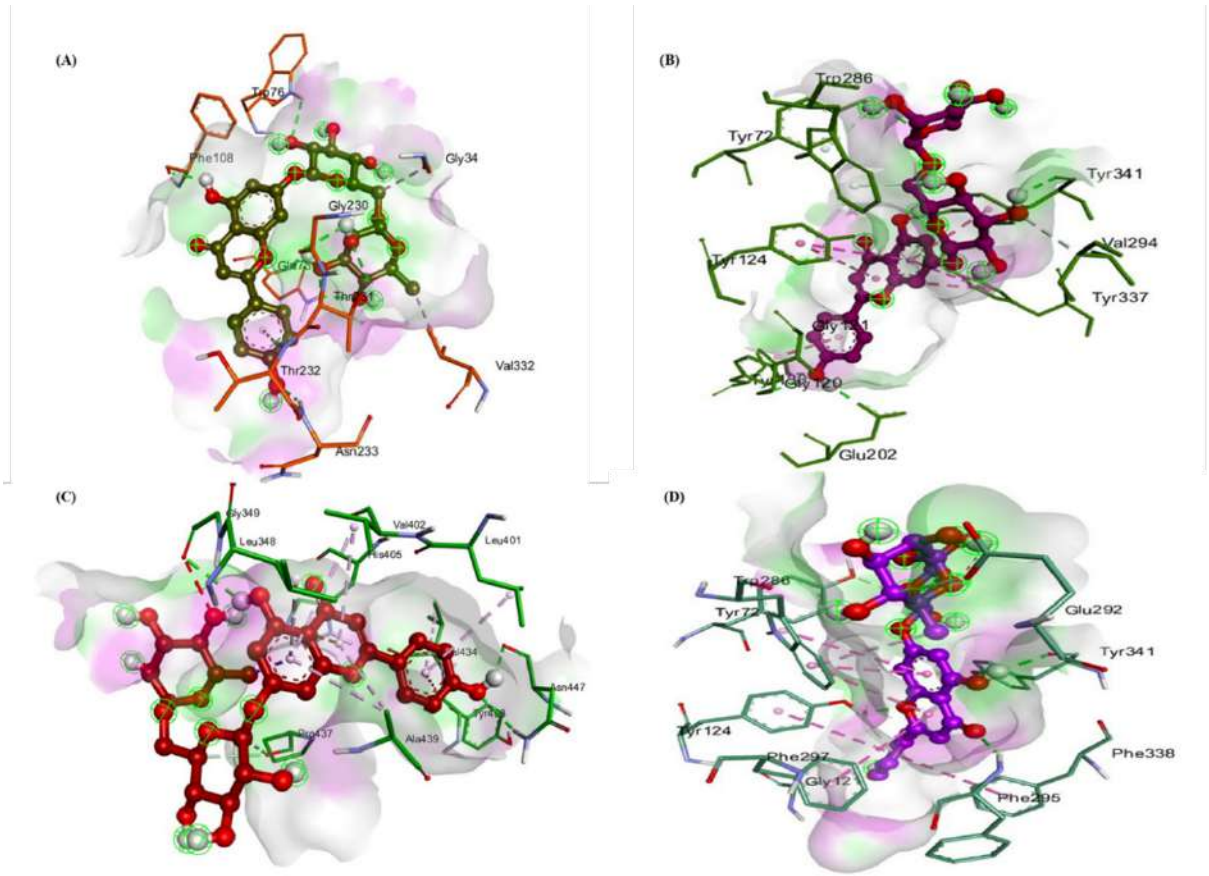


**Figure 2:** (A), (B), (C) and (D) 3D diagram of BACE1-isorhoifolin, AChE inhibitor-isorhoifolin, TNF3-isorhoifolin, and GSK3-isorhoifolin respectively.

surrounding amino acid residues at active site of AChE such as Gly121 (Convention H-bond), Tyr124 (Vander wall H-bond), Phe295 (H bond), Tyr341 ( H bond), Trp286 (pi-pi stacked T shape bond), Phe297 (pi-pi stacked T shape bond), for GSK3 active site all phytoconstituents showed binding energies ranging between -7.2 kcal/mol to -9.7 kcal/mol and isorhoifolin had highest binding energy of -9.7 kcal/mol and had interactions of amino acid residues at Val70 (pi-sigma bond), Ile62 (pi-sigma bond), Leu188 (pi-alkyl bond), Cys199 (pi-pi alkyl bond). For TACE, binding energies of phytoconstituents ranging from -7.5 kcal/mol to -9 kcal/mol and isorhoifolin shown the highest binding energy of -9 kcal/mol, and interaction of amino acid residues at Leu348 (H bond), Asp447 (H bond), Glu406 (H bond), Pro437 (H bond), Tyr433 (pi-stacked), Leu401 (pi-stacked), Val402 (pi-stacked), Val434 (pi-stacked), Ala439 (pi-stacked). The above synergy of isorhoifolin is responsible for its high binding

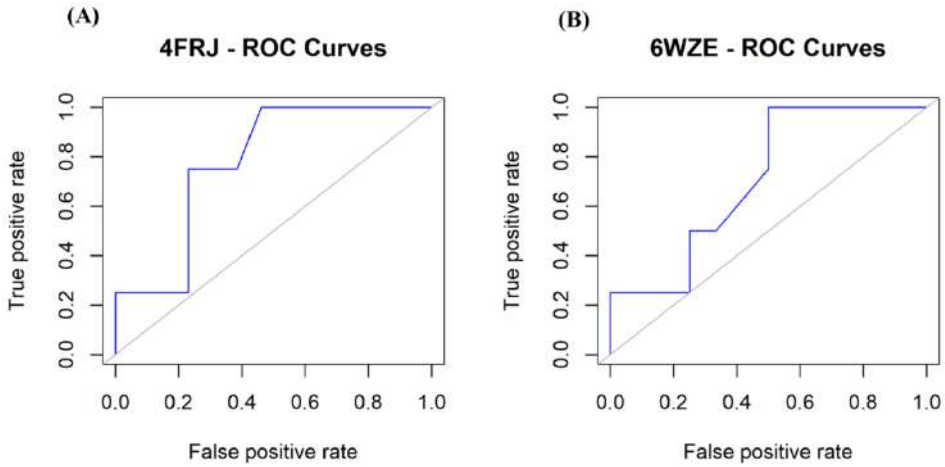


**Figure 3:** (A) and (B) ROC curves of docked complexed proteins 4FRJ and 6ZWE with isorhoifolin.

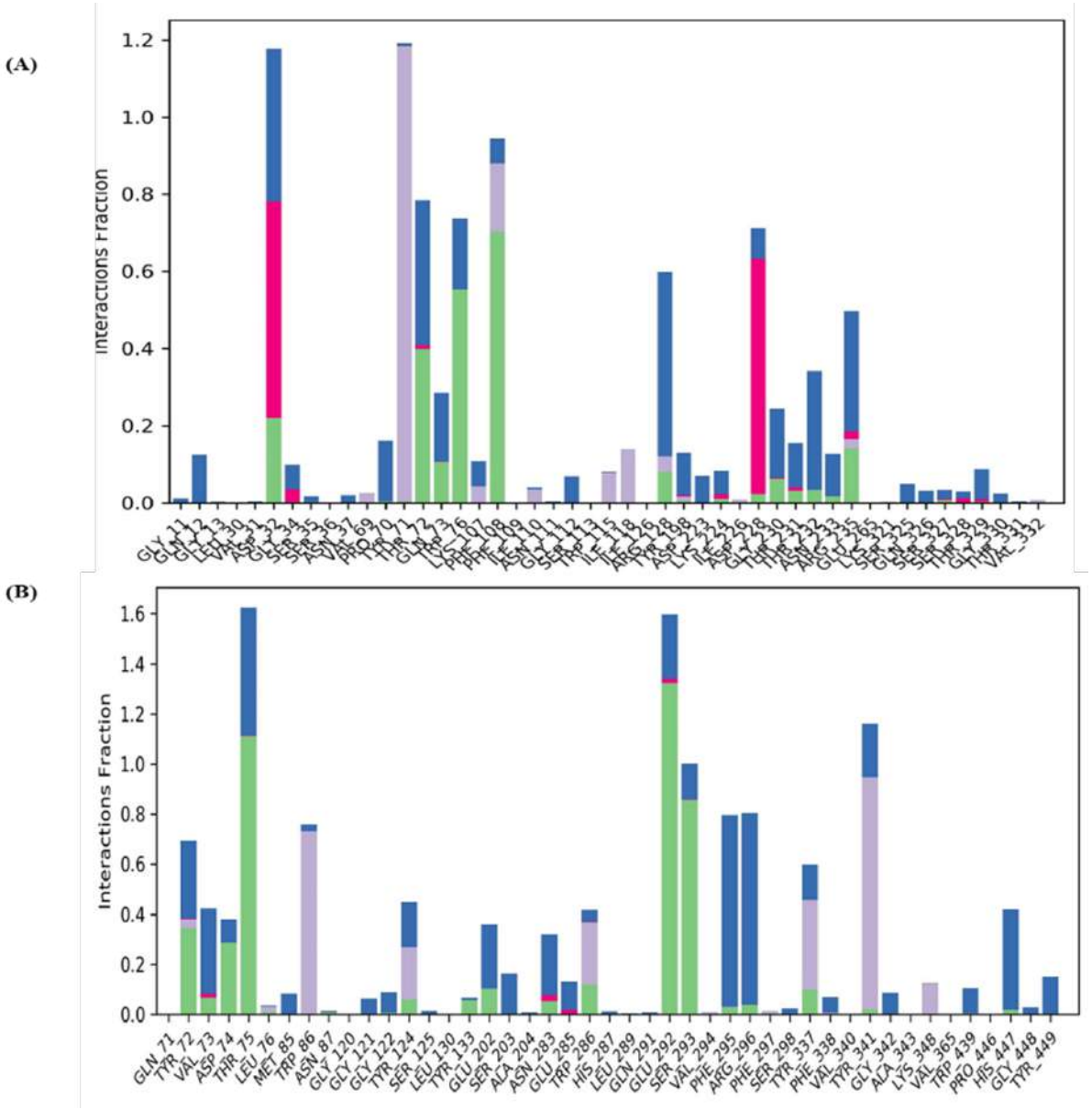


**Figure 4:** (A) and (B) Types of bond interaction of target protein complexes 4FRJ-isorhoifolin and 6ZWE-isorhoifolin respectively.

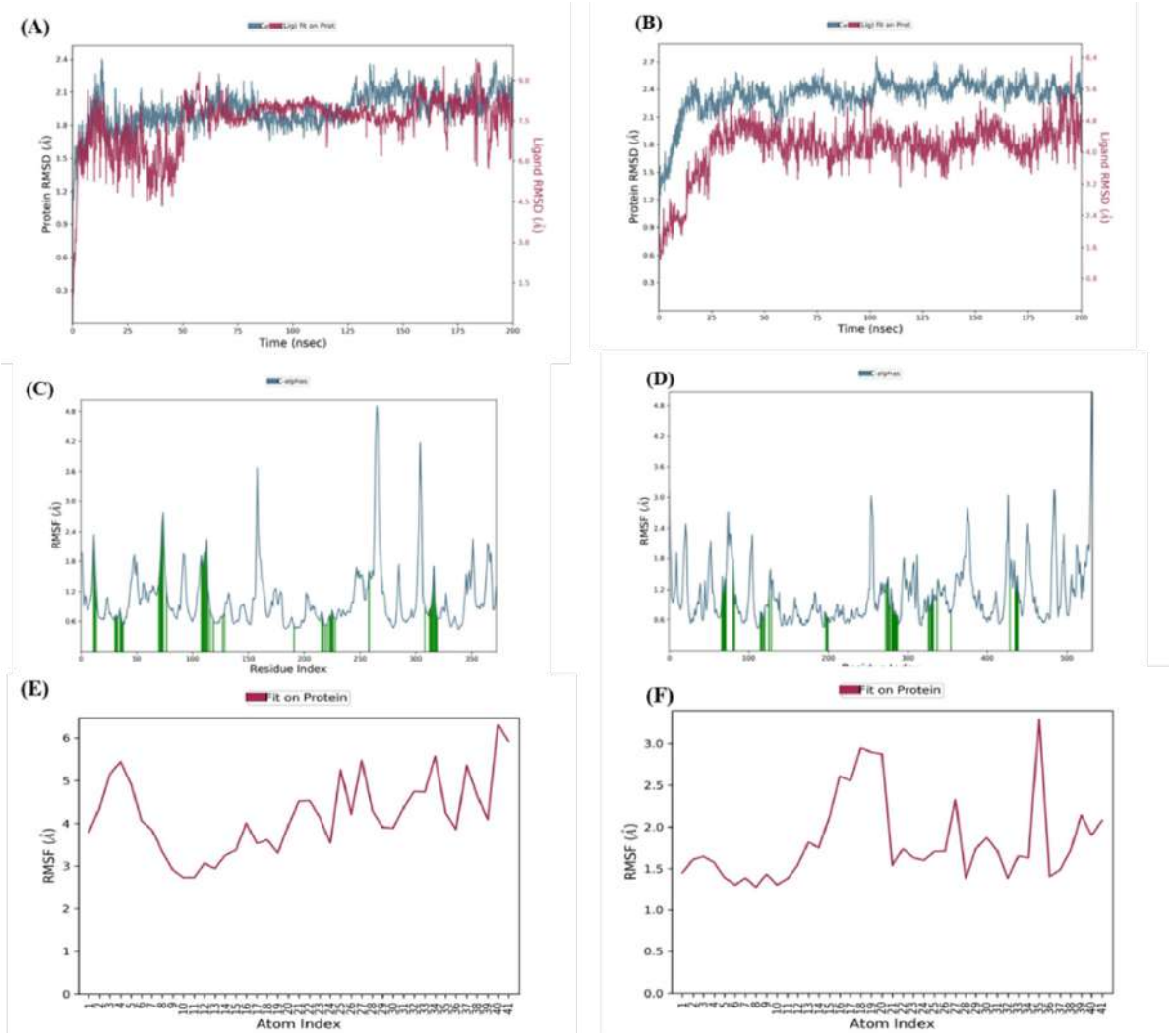


**Figure 5:** (A) and (B) protein BACE1 and AChE inhibitor RMSD with ligand isorhoifolin RMSD plot, (C) and (D) protein 4FRJ, 6ZWE RMSF plot, (E) and (F) ligand isorhoifolin RMSF. plot.

energy, contrary to the other phytochemicals of the plant (Figure 2B, 2C, and 2D). Hence, we used isorhoifolin phytoconstituent for further molecular dynamics and DFT calculation. The most stable complex for the MD simulation analysis was selected based on the binding energy of the complexes that BACE1-isorhoifolin and AChE-isorhoifolin had the highest binding energy, -10.2 and -10.9 kcal/mol, respectively. These two complexes were further analysed for docking validation and MD studies.

## Docking validation

To confirm AutoDock Vina's capability to differentiate between active and inactive molecules, a ROC curve was generated after docking isorhoifolin with their decoys against the receptor proteins AChE and BACE1, which had shown the highest binding energy with respect to those proteins. The Area under the Curve (AUC) value was calculated to evaluate the docking performance. AUC values between 0.5 and 0.7 are regarded as moderate, values larger than 0.7 as acceptable, and values less than 0.5 indicate poor discrimination ability. The docking model for the receptor demonstrated good discriminatory capacity with an AUC of 0.7788462 and 0.708333 for AChE and BACE 1 protein, respectively, indicating AutoDock Vina's efficacy in distinguishing between active compounds and decoys (Figure 3A and 3B).

## Molecular dynamics

The interaction between the proteins AChE and BACE1 with the ligand isorhoifolin was further evaluated through Molecular Dynamics (MD) simulation studies.[28] Key binding interactions, including hydrogen bonding (AChE: Thr95, Glu292, Ser293; BACE1: Gly32, Trp36, Pro108, Arg235 for), ionic interactions (Ala204, Asn283 for AChE; Asp32, Asp298 for BACE1), hydrophobic interactions (Met85, Gly122, Glu285, Tyr337, Val340 for AChE; Thr71, Ile118 for BACE1), and water-formed bridges, were analysed to evaluate binding interactions at the active sites of AChE and BACE1 individually (Figures 4A and 4B). Protein RMSF values were 2.4 Å for AChE and 1.8 Å for BACE1, while ligand RMSF values were 3 Å for AChE and 6 Å for BACE1. RMSD

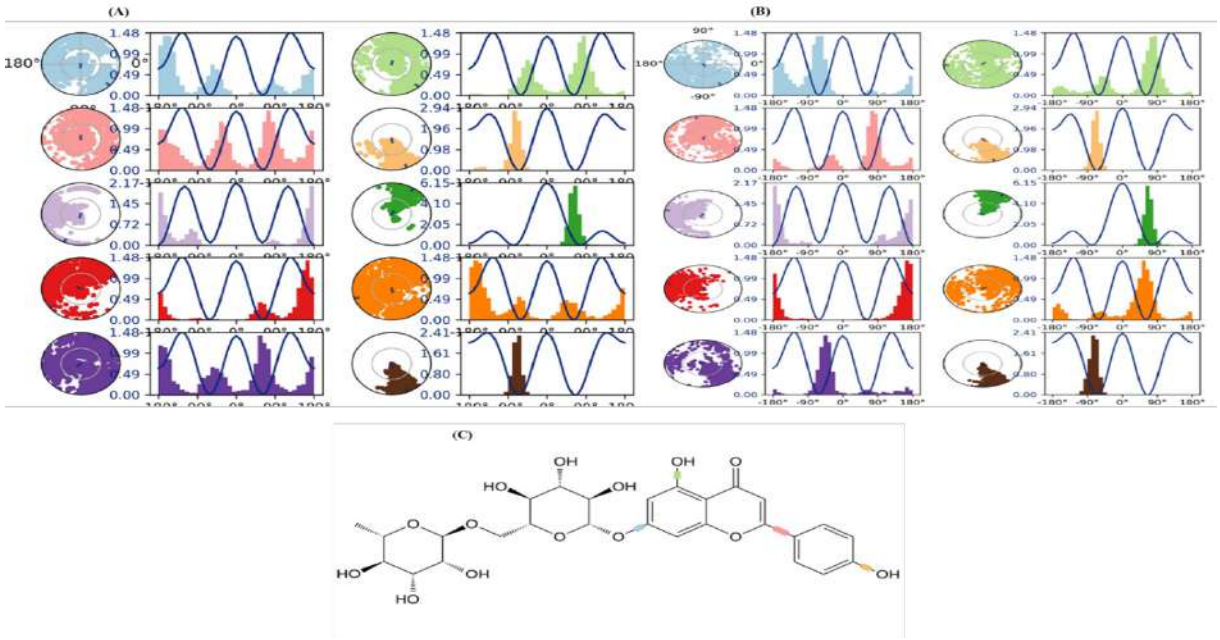


**Figure 6:** (A), (B), and (C) Isorhoifolin torsion profile concerning complex of protein 4FRJ and 6ZWE respectively.

**Table 2: ADMET profiling of isorhoifolin.**

| Sl. No. | ADMET attributes | Property name (unit) | Speculated values |
|---|---|---|---|
| 1 | Absorption | Skin permeability (log Kp) | -2.735 |
| | | Water solubility (log mol/L) | -3.262 |
| | | Caco2 permeability (LOG Papp in 10-6cm/s) | 0.392 |
| | | P-glycoprotein substrate | Yes |
| | | P-glycoprotein I inhibitor | No |
| | | P-glycoprotein II inhibitor | No |
| | | Intestinal absorption[human](%Absorbed) | 30.186 |
| 2 | Distribution | Fraction unbound [human](Fu) | 0.089 |
| | | BBB permeability (log BB) | -1.845 |
| | | CNS permeability (log PS) | -5.145 |
| | | VDss[human] (log L/kg) | 0.269 |
| 3 | Metabolism | CYP2D6 substrate | No |
| | | CYP1A2 inhibitor | No |
| | | CYP3A4 substrate | No |
| | | CYP2C19 inhibitor | No |
| | | CYP2D6 inhibitor | No |
| | | CYP2C9 inhibitor | No |
| 4 | Excretion | Renal OCT2 substrate | No |
| | | Total Clearance (log ml/min/kg) | 0.451 |
| 5 | Toxicity | Hepatotoxicity | No |
| | | Skin sensitization | No |
| | | T. Pyriformis toxicity (log ug/L) | 0.285 |
| | | Minnow toxicity (log mM) | 5.005 |
| | | Oral rat acute toxicity [$LD_{50}$] (mol/kg) | 3.903 |
| | | hERG_ I inhibition | No |
| | | hERG_II inhibition | Yes |

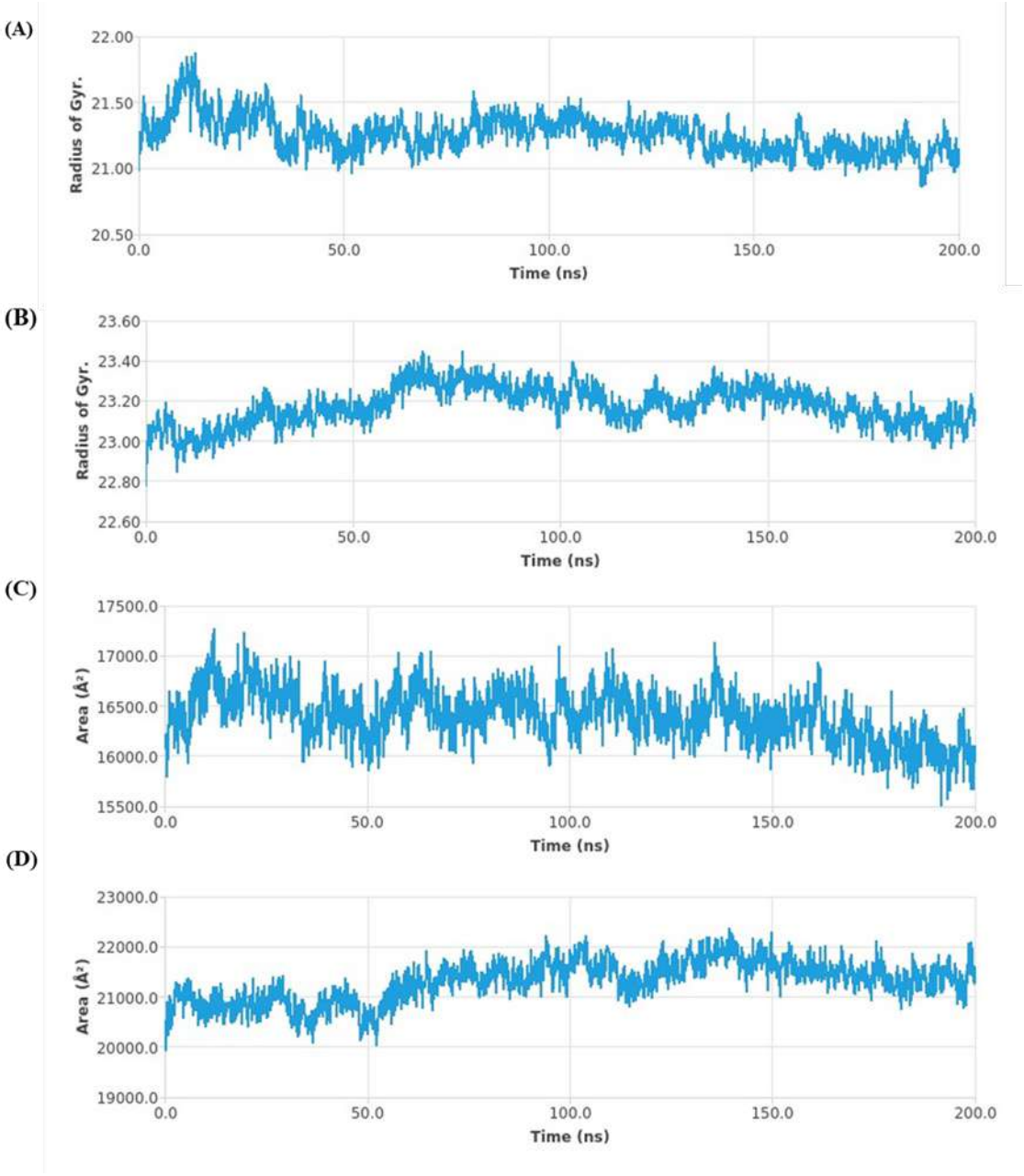


**Figure 7:** (A), (B), (C) and (D) Radius of gyration and SASA plot of target protein BACE1and AChE inhibitor with isorhoifolin complex respectively.

values were 2.8 Å for AChE, 1.8 Å for BACE1, and ligand RMSD values were 1.8 Å for AChE and 1.5 Å for BACE1 (Figures 5A, 5B, 5C, 5D, 5E, and 5F). These results indicated that isorhoifolin interactions are stable up to 200 ns at the AChE site. Similarly, the BACE1-isorhoifolin complex showed an ideal interaction profile of up to 200 ns. These simulation studies suggest that isorhoifolin forms various key interactions and resides well at the active sites of AChE and BACE1. The median radius of Gyration (rGyr) for the BACE1-isorhoifolin and AChE-isorhoifolin complexes was 22 $Å^2$ and 23.2 $Å^2$, respectively, throughout the 200 ns MD simulation (Figures 7A, 7B, 7C, 7D). Ligand torsion analysis revealed that isorhoifolin possesses four rotatable bonds within its phenyl aliphatic ring, impacting the energy dynamics of ligand binding. This was visualized using dial and bar plots, where each rotatable bond's torsional angle was tracked throughout the simulation (Figures 6A, 6B, and 6C). Hydrogen bonds, crucial for drug design, were observed in the protein-ligand binding, involving backbone and side-chain donors and acceptors. Additionally, the Solvent-Accessible Surface Area (SASA) decreased after the ligand was bound to the target proteins, further supporting the stability of the complexes. Overall, the interaction stability, as indicated by the consistent rGyr values, suggests a strong and stable binding of isorhoifolin to AChE and BACE1 over the 200 ns simulation period (Figures 7A, 7B, 7C, and 7D).

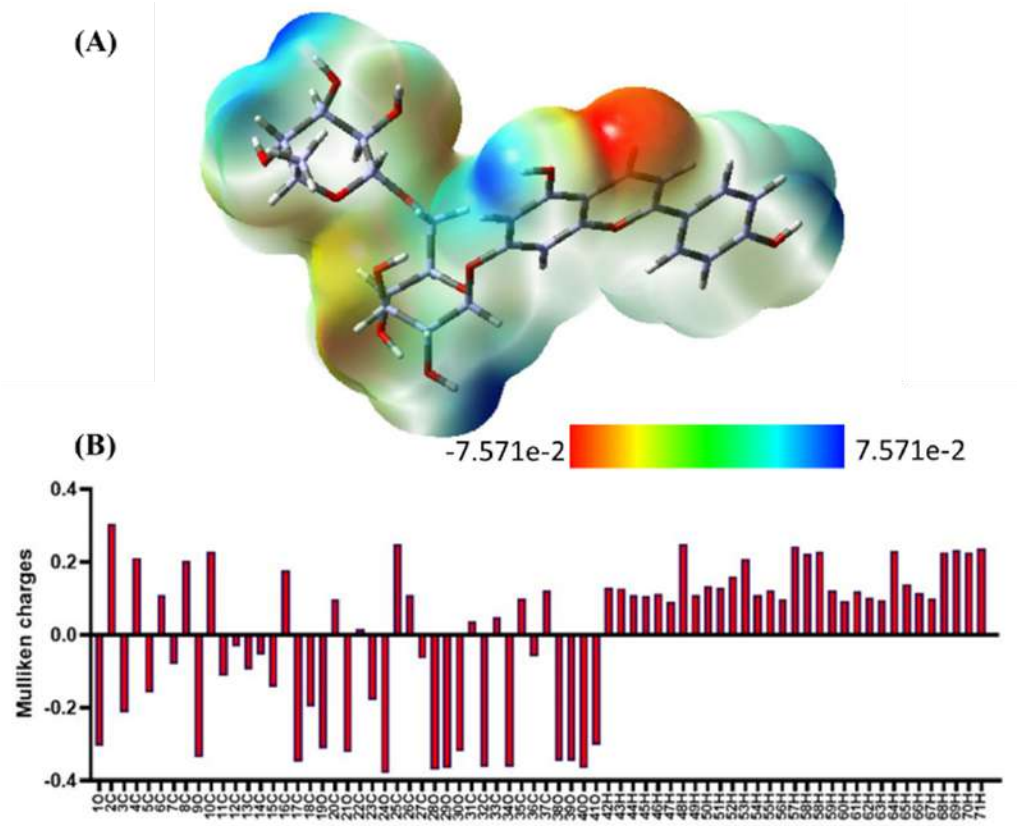


**Figure 8:** (A) Molecular Electrostatic Potential (MEP) surface of isorhoifolin. (B) Illustration showing mulliken charges of each atom of isorhoifolin

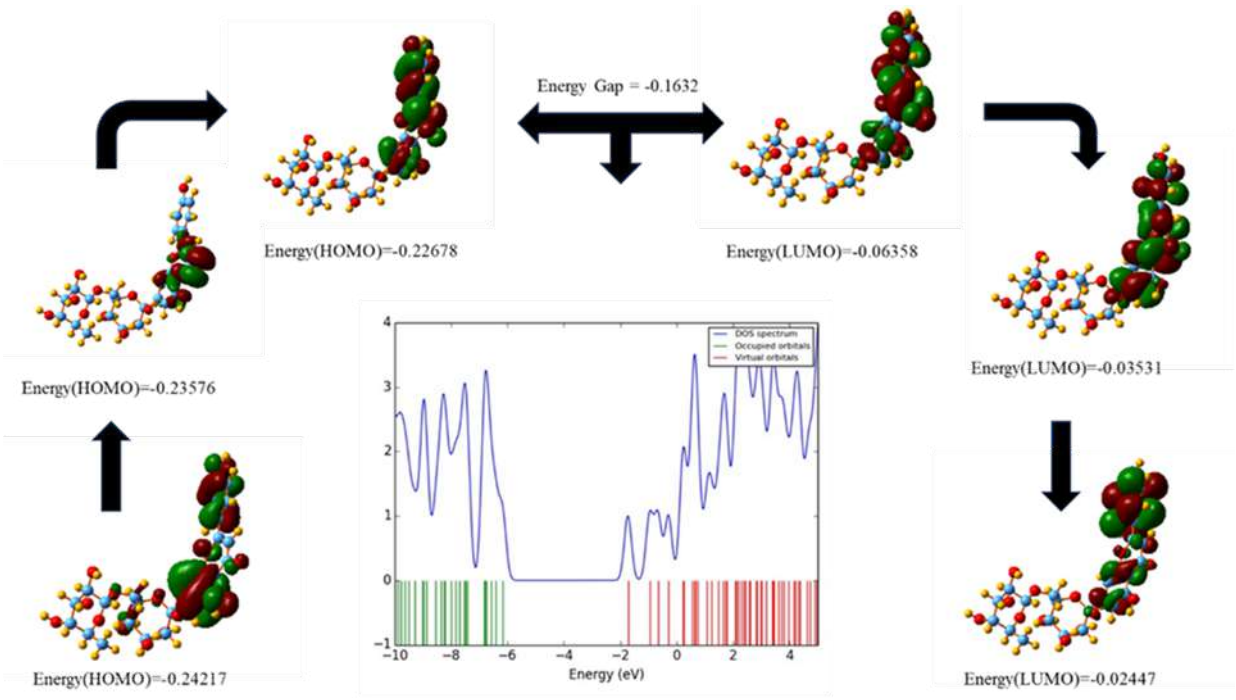


**Figure 9:** HOMO-LUMO energy split and DOS spectra of isorhoifolin.

## Density Functional Theory (DFT) studies

DFT studies were conducted to optimize the structure of isorhoifolin (Figure 3A). Bond lengths and angles of individual atoms were determined, revealing a C=O bond length of 1.5 Å and a C-H bond length of 2 Å. MEP surface analysis identified electrophilic and nucleophilic sites (Figure 8A). The charge distribution on the MEP surface was depicted with colours

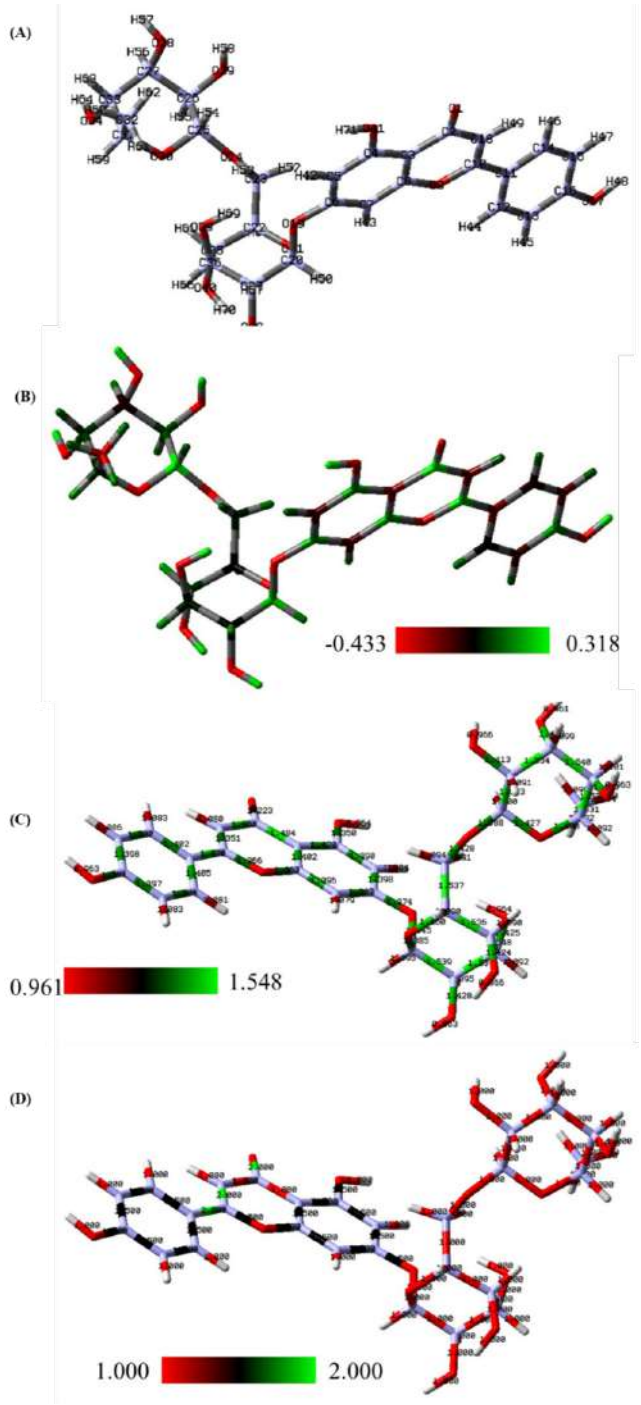


**Figure 10:** (A) Optimised structure of isorhoifolin, (B) Colour-charged representation of isorhoifolin. (C) and (D) Bond length and bond order values illustration of atoms of isorhoifolin.

ranging from red (most negative electrostatic potential) to blue (most positive electrostatic potential), spanning from $-5.883\times10^{-2}$ to $5.883\times10^{-2}$. Oxygen atoms exhibited electrophilic reactivity with high electromagnetic potential, while carbon atoms showed nucleophilic reactivity (Figure 8). Frontier Molecular Orbitals (FMOs), including the Highest Occupied Molecular Orbital (HOMO) and the Lowest Unoccupied Molecular Orbital (LUMO), were analysed to understand the thermal, electrical, and chemical properties of isorhoifolin. The Density of State (DOS) spectra revealed an energy gap of 0.162 eV between the HOMO and LUMO of the test compound (Figure 9). This HOMO-LUMO energy difference suggests that isorhoifolin is highly reactive (E=EHOMO-ELUMO=0.162 eV; Figure 9). The stabilized LUMO energy indicates potential strong biological activity, likely due to the presence of electron-withdrawing carbonyl groups. Mullikan charges, bond lengths, and bond orders were calculated using Gaussian software 6.0.16 (Figure 10). The results suggest that isorhoifolin has a high tendency to absorb electrons. Hydrogen and carbon atoms displayed positive charges, whereas oxygen atoms showed negative charges. The analysis revealed numerous electrophilic sites, indicating that isorhoifolin is highly reactive in biological systems. Additionally, the bond orders and lengths were assessed to evaluate the stability of isorhoifolin.

## ADMET Attributes

The physical properties, drug-likeness, ADME (Absorption, Distribution, Metabolism, and Excretion), and toxicity profile of isorhoifolin were evaluated using pkCSM servers (Table 2). Isorhoifolin exhibited drug-like properties in accordance with Lipinski's rule of five. It demonstrated human intestinal absorption and showed permeability in MDCK and Caco-2 cell lines, suggesting that it can be administered orally. In addition, toxicity prediction results suggested that isorhoifolin was predicted to have no toxicity in mice and rats. The cardiotoxicity (hERG) prediction indicates low risk against the hERG channel. The *in silico* predicted results are presented in the Table 2.

## CONCLUSION

Alzheimer's disease treatment is a complex challenge, with current treatments offering only symptomatic relief. A promising avenue is multi target pharmacology aiming to simultaneously target multiple aspects of the disease. Botanical drugs show potential in this approach, offering hope for more effective treatments. The current study investigated few phytoconstituents of *Gmelina asiatica* known for their reported neuroprotective activity in the literature against four targets, AChE, BACE1, GSK-3, and TACE1, by computational docking. Among these, isorhoifolin identified promising phytoconstituent having good binding energy and noteworthy interaction at the active site of proteins. Molecular dynamics simulations confirmed the stability of isorhoifolin's complexes over a 200 ns period. Additionally, Density Functional Theory (DFT) studies revealed its chemical and structural reactivity. Additionally, Density Functional Theory (DFT) studies indicated favourable structural properties and reactivity of isorhoifolin. ADMET properties assessment revealed its promising drug-likeness and safety profile. This study provides important insight into isorhoifolin's potential as a multi-target candidate for Alzheimer's disease and demands further *in vitro* and *in vivo* investigations for lead optimization and validation.

## ACKNOWLEDGMENT

I, (Komal Rajesh Andarghiske) thankful to MHRD, India and Indian Institute of Technology (Banaras Hindu University), Varanasi for providing a fellowship.

## CONFLICT OF INTEREST

The authors declare that there is no conflict of interest.

## ABBREVIATIONS

**AD:** Alzheimer's disease; **DFT:** Density functional theory; **HOMO:** Highest occupied molecular orbital; **LUMO:** Lowest occupied molecular orbital; **RMSD:** Root mean square deviation; **RMSF:** Root mean square deviation; **RG:** Radius of gyration; **SASA:** Solvent accessible surface area; **Aβ:** amyloid-beta; **APP:** Amyloid processing protein; **NFT:** Neurofibrillary tangles; **GSK-3:** Glycogen synthase kinase-3; **TACE:** TNF-alpha converting enzyme; **BACE:** Enzyme cleaves APP at β-site; **IMMPAT:** Indian Medicinal Plants Phytochemistry therapeutics database.

## SUMMARY

In this study, *Gmelina asiatica* constituents' activity was evaluated through various *in silico* studies, i.e., molecular docking, molecular dynamics simulations and DFT studies. The docking studies suggested that isorhoifolin is a hit compound. Further, molecular dynamics simulations and DFT studies also supported the isorhoifolin is stable and has significant electrochemical properties in the interaction of AChE, BACE1, GSK-3, and TACE1 proteins for the management of Alzheimer's disease.

## REFERENCES

1. Karakaya S, Koca M, Yılmaz SV, Yıldırım K, Pınar NM, Demirci B, *et al.* Molecular Docking Studies of Coumarins Isolated from Extracts and Essential Oils of *Zosima absinthifolia* Link as Potential Inhibitors for Alzheimer's disease. Molecules. 2019;24(4):722. doi: 10.3390/molecules24040722, PMID 30781573.
2. Barai P, Raval N, Acharya S, Borisa A, Bhatt H, Acharya N. Neuroprotective effects of bergenin in Alzheimer's disease: investigation through molecular docking, *in vitro* and *in vivo* studies. Behav Brain Res. 2019;356:18-40. doi: 10.1016/j.bbr.2018.08.010, PMID 30118774.
3. Elangovan ND, Dhanabalan AK, Gunasekaran K, Kandimalla R, Sankarganesh D. Screening of potential drug for Alzheimer's disease: a computational study with GSK-3 β inhibition through virtual screening, docking, and molecular dynamics simulation. J Biomol Struct Dyn. 2021;39(18):7065-79. doi: 10.1080/07391102.2020.1805362, PMID 32779973.
4. Tettevi EJ, Kuevi DN, Sumabe BK, Simpong DL, Maina MB, Dongdem JT, *et al. In silico* Identification of a Potential TNF-Alpha Binder Using a Structural Similarity: A Potential Drug Repurposing Approach to the Management of Alzheimer's disease. BioMed Res Int. 2024;2024(1):9985719. doi: 10.1155/2024/9985719, PMID 38221912.
5. Gandham SK, Chintha VR, Wudayagiri R. *In silico* evaluation of Benzo (f) chromen-3-one as a potential inhibitor of NF-κB: a key regulatory molecule in inflammation-mediated pathogenesis of diabetes, Alzheimer's, and cancer. J App Pharm Sci. 2018;8(12):157-64. doi: 10.7324/JAPS.2018.81218.
6. Khan MB, Palaka BK, Sapam TD, Subbarao N, Ampasala DR. Screening and analysis of acetyl-cholinesterase (AChE) inhibitors in the context of Alzheimer's disease. Bioinformation. 2018;14(8):414-28. doi: 10.6026/97320630014414, PMID 30310249.
7. Huang XY, Li TT, Zhou L, Liu T, Xiong LL, Yu CY. Analysis of the potential and mechanism of *Ginkgo biloba* in the treatment of Alzheimer's disease based on network pharmacology. Ibrain. 2021;7(1):21-8. doi: 10.1002/j.2769-2795.2021.tb00060.x, PMID 37786872.
8. Melnikova I. Therapies for Alzheimer's disease. Nat Rev Drug Discov. 2007;6(5):341-2. doi: 10.1038/nrd2314, PMID 17539055.
9. Wang W, Bodles-Brakhop M. A, W Barger S. A role for P-glycoprotein in clearance of Alzheimer amyloid β-peptide from the brain. Curr Alzheimer Res. 2016;13(6):615-20.
10. Asher S, Priefer R. Alzheimer's disease failed clinical trials. Life Sci. 2022;306:120861. doi: 10.1016/j.lfs.2022.120861, PMID 35932841.
11. Yiannopoulou KG, Anastasiou AI, Zachariou V, Pelidou SH. Reasons for failed trials of disease-modifying treatments for Alzheimer disease and their contribution in recent research. Biomedicines. 2019;7(4):97. doi: 10.3390/biomedicines7040097, PMID 31835422.
12. León R, Garcia AG, Marco-Contelles J. Recent advances in the multitarget-directed ligands approach for the treatment of Alzheimer's disease. Med Res Rev. 2013;33(1):139-89. doi: 10.1002/med.20248, PMID 21793014.
13. Albertini C, Salerno A, de Sena Murteira Pinheiro P, Bolognesi ML. From combinations to multitarget-directed ligands: A continuum in Alzheimer's disease polypharmacology. Med Res Rev. 2021;41(5):2606-33. doi: 10.1002/med.21699, PMID 32557696.
14. Oyinloye BE, Iwaloye O, Ajiboye BO. Polypharmacology of *Gongronema latifolium* leaf secondary metabolites against protein kinases implicated in Parkinson's disease and Alzheimer's disease. Sci Afr. 2021;12:e00826. doi: 10.1016/j.sciaf.2021.e00826.
15. Ksirri R, Khazem M, Bhanukiran K, Hemalatha S. G melina asiatica: exploring traditional uses, pharmacological insights, and phytoconstituents-comprehensive review (1961-2023). Phytochem Rev. 2024:1-24.
16. Florence A, Rosy BA, Judisha DM. A Review on Pharmacological properties of *Gmelina asiatica* L. Common Medicinal Plants of our surroundings. Vol. 48; 2024.
17. Shanmugalingam V, SATHASİVAMPİLLAİ SV, SEBASTİAN PR. Biological activities of extracts of *Gmelina asiatica* L. Doğu Fen bilimleri. Dergisi. 2022;5(1):1-13.
18. Ksirri R, Bhanukiran K, Maity S, Maiti P, Hemalatha S. Evaluation of anticancer activity of *Gmelina asiatica* leaves, *in vitro* and *in silico* studies. J Biomol Struct Dyn. 2023:1-16.
19. Nour H, Abdou A, Belaidi S, Jamal J, Elmakssoudi A, Dakir M, *et al.* Discovery of promising cholinesterase inhibitors for Alzheimer's disease treatment through DFT, docking, and molecular dynamics studies of eugenol derivatives. J Chin Chem Soc. 2022;69(9):1534-51. doi: 10.1002/jccs.202200195.
20. Merlin N, Parthasarathy V, Manavalan R, Kumaravel S. Chemical investigation of aerial parts of *Gmelina asiatica* Linn by GC-MS. Pharmacogn Res. 2009;1(3).
21. Chlebek J, Korábečný J, Doležal R, Štěpánková Š, Pérez DI, Hošťálková A, *et al. In vitro* and *in silico* acetylcholinesterase Inhibitory Activity of Thalictricavine and Canadine and Their Predicted Penetration across the blood-brain Barrier. Molecules. 2019;24(7). doi: 10.3390/molecules24071340, PMID 30959739.
22. Basu A, Sarkar A, Maulik U. Molecular docking study of potential phytochemicals and their effects on the complex of SARS-CoV2 spike protein and human ACE2. Sci Rep. 2020;10(1):17699. doi: 10.1038/s41598-020-74715-4, PMID 33077836.
23. Garg S, Anand A, Lamba Y, Roy A. Molecular docking analysis of selected phytochemicals against SARS-CoV-2 Mpro receptor. Vegetos. 2020;33(4):766-81. doi: 10.1007/s42535-020-00162-1, PMID 33100613.
24. Seniya C, Khan GJ, Uchadia K. Identification of potential herbal inhibitor of acetylcholinesterase associated Alzheimer's disorders using molecular docking and Molecular Dynamics simulation. Biochem Res Int. 2014; 2014:705451. doi: 10.1155/2014/705451, PMID 25054066.
25. Akawa OB, Subair TI, Soremekun OS, Olotu FA, Soliman ME. Structural alterations in the catalytic core of hSIRT2 enzyme predict therapeutic benefits of *Garcinia mangostana* derivatives in Alzheimer's disease: molecular dynamics simulation study. RSC Adv. 2021;11(14):8003-18. doi: 10.1039/d0ra10459k, PMID 35423339.
26. Bhanukiran K, Singh R, T A G, Ramakrishna K, Singh SK, Krishnamurthy S, *et al.* Vasicinone, a pyrroloquinazoline alkaloid from *Adhatoda vasica* Nees enhances memory and cognition by inhibiting cholinesterases in Alzheimer's disease. Phytomed Plus. 2023;3(2):100439. doi: 10.1016/j.phyplu.2023.100439.
27. Kumar S, Chowdhury S, Kumar S. *In silico* repurposing of antipsychotic drugs for Alzheimer's disease. BMC Neurosci. 2017;18(1):76. doi: 10.1186/s12868-017-0394-8, PMID 29078760.
28. Khare N, Maheshwari SK, Jha AK. Screening and identification of secondary metabolites in the bark of *Bauhinia variegata* to treat Alzheimer's disease by using molecular docking and molecular dynamics simulations. J Biomol Struct Dyn. 2021;39(16):5988-98. doi: 10.1080/07391102.2020.1796798, PMID 32720564.

**Cite this article:** Andarghiske KR, Bhanukiran K, Hemalatha S. *In silico* Exploration of *Gmelina asiatica* for Multitarget Neuroprotection in Alzheimer's Disease. Pharmacog Res. 2025;17(1):115-25.